School of Electrical Engineering & School of Science

Simultaneous EEG and fMRI: T1-based evaluation of heating in a gel phantom at 3 Tesla

Iina E. Aaltonen neé Tarnanen,
Raimo E. Sepponen,
Veikko T. Jousmäki

Aalto University | SCIENCE + TECHNOLOGY | TECHNICAL REPORT

Aalto University publication series
SCIENCE + **TECHNOLOGY** 22/2012

Simultaneous EEG and fMRI: T1-based evaluation of heating in a gel phantom at 3 Tesla

Iina E. Aaltonen neé Tarnanen, Raimo E. Sepponen, Veikko T. Jousmäki

Aalto University
School of Electrical Engineering, School of Science
Department of Electronics & OV Lounasmaa Laboratory
& Advanced Magnetic Imaging Centre

Aalto University publication series
SCIENCE + **TECHNOLOGY** 22/2012

ISBN 978-952-60-4959-5 (pdf)
ISSN-L 1799-4896
ISSN 1799-4896 (printed)
ISSN 1799-490X (pdf)
http://urn.fi/URN:ISBN:978-952-60-4959-5

Unigrafia Oy
Helsinki 2012

Finland

Author

Author(s):Iina E. Aaltonen neé Tarnanen, Raimo E. Sepponen, Veikko T. Jousmäki

Name of the publication

Simultaneous EEG and fMRI: T1-based evaluation of heating in a gel phantom at 3 Tesla

Publisher School of Electrical Engineering & School of Science

Unit Department of Electronics, OV Lounasmaa Laboratory & Advanced Magnetic Imaging Centre

Series Aalto University publication series SCIENCE + TECHNOLOGY 22/2012

Field of research Functional Imaging

Abstract

EEG electrodes and leads, comparable to metallic implants, can lead to heating of tissue when used in an MRI scanner. Simultaneous EEG and fMRI experiments are frequently carried out at 3 T or higher fields. High field strength, and thus high-energy RF pulses, added to complex EEG lead configuration increases the risk of severe localized heating, or hot spots. Unlike the skin, the brain lacks thermoreceptors, and the subject might not report anything unusual during the scan although hot spots may occur.

In simultaneous EEG and fMRI experiments, the temperature at individual electrode sites can be monitored using optic fibre temperature probes. To complement the isolated surface temperature readings, we aimed to map the whole temperature distribution within a phantom. An EEG-equipped gel phantom was imaged using a T1-weighted sequence before and after running a high-energy MR sequence at 3 T. Changes in T1 intensity profile would indicate a relative temperature increase.

In our setting, hot spots were not detected in the relative temperature maps of the phantom. Optic fibre temperature probes at selected electrode sites indicated small temperature increases depending on the MR sequence used. The phantom core temperature remained unchanged.

RF energy distribution can vary with electrode configurations and MRI scanners. We suggest that EEG equipments should be tested for safety reasons. The MRI thermometry –inspired relative T1 intensity method provides an easy way to test possible heating within a phantom.

Keywords 3T, functional magnetic resonance imaging, electroencephalography, heating

ISBN (printed)	**ISBN (pdf)** 978-952-60-4959-5	
ISSN-L 1799-4896	**ISSN (printed)** 1799-4896	**ISSN (pdf)** 1799-490X
Location of publisher Espoo	**Location of printing** Helsinki	**Year** 2012
Pages 20	**urn** http://urn.fi/URN:ISBN:978-952-60-4959-5	

1. Introduction

In magnetic resonance (MR) imaging experiments the subject is exposed to static, gradient, and radio frequency (RF) magnetic fields. Upper limits have been set to these field strengths to prevent undesired effects such as nerve stimulation and tissue heating (ICNIRP, 1998, 2004).

These limits, however, cannot take into account unpredictable localized RF energy concentrations, hot spots, which can occur when conducting objects are brought into the vicinity of the subject (Shellock, 2000). Unlike in the skin, thermoreceptors are absent in brain tissue, and thus hot spots are especially dangerous.

The rate at which RF energy is absorbed into the tissue is described by specific absorption rate (SAR) defined as absorbed power divided by mass of tissue (ICNIRP, 2004). Typically, SAR is calculated as an average over a 6-minute period. In the head, the partial body SAR should not exceed 3 W/kg and the corresponding temperature should not exceed 38°C in normal operating mode.

The heating of metallic implants has been extensively studied (Dempsey and Condon, 2001; Shellock 2001, 2002). However, only a few research groups have reported of temperature measurements concerning simultaneous EEG and fMRI measurements after Lemieux et al. (1997) reported of heating of unattached EEG electrodes.

Temperature has been measured from individual EEG electrode sites using temperature probes from volunteers (Lazeyras et al., 2001), a sheep head (Meriläinen, 2002), and a saline or gel phantom (Mirsattari et al., 2004; Stevens et al., 2007; Mullinger et al., 2008). The first two of these studies, and an intracranial-EEG-fMRI study (Carmichael et al., 2010), found significantly increased temperatures when MR sequences with high SAR values were used.

Angelone et al. (2004) simulated the effect of electrodes and leads on SAR distribution within the brain using a realistic, high resolution head model obtained from individual MR images. They reported that heating was most prominent on the skin and SAR was found to increase with the number of electrodes because the homogeneity of the magnetic field was perturbed

more. A later study by Angelone et al. (2006) also investigated the effect of electrode lead resistivity on heating using both simulations and optic fibre probes.

Simulations and temperature probes provide valuable information about heating although they are unsuitable for practical simultaneous EEG and fMRI experiments where the configuration of multiple EEG electrodes and leads can easily result in undesired hot spots. Temperature changes within tissue can, however, be mapped non-invasively using MR thermometry.

MRI thermometry methods include the water proton resonance frequency (PRF), diffusion coefficient, MR spectroscopic imaging (MRSI), and longitudinal relaxation time (T1) dependent methods (Wlodarczyk et al., 1999; de Senneville et al., 2005). Each of these methods have their advantages and drawbacks related to imaging time, resolution, and artefacts. PRF has been used to monitor heating of conductive wires within a phantom (Ehses et al., 2008). However, the authors acknowledged that susceptibility artefacts might prevent this thermometry method from being used with some implants.

T1 relaxation time is dependent on temperature (Bloembergen et al., 1948). When the temperature change is small, the relationship can be approximated linear (de Senneville et al., 2005). In T1-weighted images the temperature change is seen as a relative change in voxel intensity.

The aim of this study is to implement and report on a simple safety evaluation procedure which includes temperature monitoring from an agar-saline balloon phantom using optic fibre temperature probes and an MRI thermometry –inspired relative T1-intensity method. The procedure is described in detail, and the results of the simultaneous EEG and fMRI recordings are reported.

2. Materials and methods

2.1 Equipment

2.1.1 EEG system

Our EEG system consists of a 32-channel MR-compatible amplifier and a customized 32-channel electrode cap (BrainAmp MR Plus; BrainCap MR with three EOG and one ECG Ag/AgCl electrodes with 5-kΩ current-limiting resistors; BrainProducts GmbH, Munich, Germany). The connectors of the detachable EOG and ECG electrodes have been changed in-house to reduce susceptibility artefacts. Susceptibility artefacts of the non-ferromagnetic EEG cap components and electrode paste (Abralyt 2000, EasyCap GmbH, Herrsching-Breitbrunn, Germany) extend typically 10 mm or less into a standard phantom in -weighted GRE-EPI images.

2.1.2 MRI scanner

The long-bore MRI scanner (GE Signa 3.0 T with Excite, Milwaukee, WI, USA) with an 8-channel receiving head coil (8HRBRAIN). The body coil is used for RF transmission.

2.1.3 Optic fibre temperature probes

Optic fibre temperature measurements were carried out using a Universal Multichannel Instrument fibre optic signal conditioner with 4 optic fibres (FISO Technologies Inc., Sainte-Foy, Canada). The method is based on Fabry-Pérot interferometer.

2.1.4 Phantoms

Two spherical phantoms were used in the measurements, first a standard GE gel phantom (Silicon filled TLT Head, Ø 17 cm) and later a self-constructed gel balloon phantom with dielectric properties resembling those of blood (ε_{gel}=78, σ_{gel}=1.52 S/m at 128 MHz). The agar-saline gel balloon phantom (Figure 1) was constructed using 5 litres of 0.9 % physiological saline and 50 grams of agar. The mixture was boiled, inserted

into a large balloon and finally cooled, resulting in a semi-solid gel-like substance.

In all experiments, the subject (phantom) weight in the MRI scanner was set to 75 kg. The EEG cap was stretched over the specified phantom and the electrode wells were filled with electrode paste. The thin dielectric layer of balloon has low impedance at RF, and therefore the coupling is quite similar to the coupling through intact skin (Schanne and Chaffin, 1970).

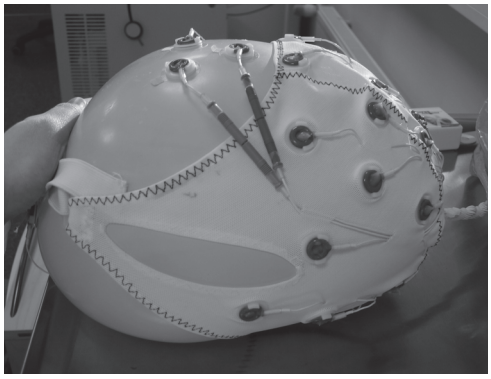

Figure 1 EEG cap with detachable EOG electrodes stretched over agar-saline balloon phantom. Electrode wells are filled with electrode paste.

2.2 Evaluation of heating using optic fibre temperature probes

Safety studies using a previous version of our EEG system (BrainProducts GmbH) showed significant temperature increases at several electrode sites (Meriläinen, 2002). Our aim was to develop a safety test for the current system including a newer version of the EEG amplifier, EEG cap with current-limiting resistors and in-house electrode connectors, and a new MRI head-coil.

First, temperature was recorded from the electrode paste of the electrode wells when the standard GE gel phantom was equipped with our current EEG system. A high-SAR MR sequence FLAIR (Parameters: TR 1000, TE minFull, TI 600, 256x256 matrix size, slice thickness 3.0, spacing 0.0, FOV 20 cm, frequency-encode direction A/P, NEX 1.00, number of slices 57 (axial); scanner-reported SAR values: Estimated SAR 1.7 W/kg, Peak SAR 3.3 W/kg) was run. All electrode sites except the very posterior ones were measured in this manner. The fibres were too brittle to accommodate to the bending pressure that would be directed at the fibres when placed to the electrode sites under the phantom.

Since modest temperature increase (0–1.3°C) was detected at most of the electrode sites using the GE phantom, we constructed the more realistic

balloon phantom as described earlier. We chose to record temperature from two electrode sites and from the balloon phantom core during 30-minute runs of three MRI sequences: GRE-EPI (Flip angle 60°C; scanner-reported Estimated SAR 0.1 W/kg, Peak SAR 0.2 W/kg), SPGR (scanner-reported Estimated SAR 0.2 W/kg, Peak SAR 0.4 W/kg), and IR (scanner-reported Estimated SAR 2.0 W/kg, Peak SAR 3.9 W/kg). The electrode sites were upper left EOG chosen based on the GE phantom recordings and FC1 (international 10–20 system) as control.

2.3 Evaluation of heating using relative T1-intensity method

The T1 relaxation time dependent method, unlike most of the MRI thermometry methods, does not suffer from susceptibility artifacts and is thus unfeasible to use with our EEG system. Since a full-scale T1 measurement is very time consuming, we decided to settle for a relative temperature map obtained by comparing the intensities of two T 1-weighted IR images taken before and after a 'heating' sequence FLAIR. Table 1 clarifies the steps taken to image the balloon phantom.

Table 1. Relative T1-intensity method summarized. Step 3 images were subtracted from Step 1 images to calculate relative temperature changes.

Phase	Purpose	MR sequence
Step 1	T1-weighted reference image at room temperature	IR
Step 2	Heating	FLAIR
Step 3	T 1-weighted image of heated phantom, cf. Step 1.	IR

The balloon phantom was surrounded by a thin plastic bag to restrain heat exchange due to air flow. IR sequence parameters: TR 1500, TE minFull, TI 700, 256x192 matrix size, slice thickness 3.0 mm, spacing 1.0 mm, field of view (FOV) 22 cm, frequency-encode direction A/P, NEX 0.75, number of slices 55 (axial); scanner-reported Estimated SAR 1.8 W/kg, Peak SAR 3.6 W/kg; Adiabatic fast passage (AFP) by default to insure full inversion.

FLAIR parameters: TR 1000, TE minFull, TI 600, 256x256 matrix size, slice thickness 2.0, spacing 0.0, FOV 22 cm, frequency-encode direction A/P, NEX 1.00, number of slices 109 (axial); scanner-reported Estimated SAR 1.6 W/kg, Peak SAR 3.2 W/kg.

2.3.1 Image processing

The T1-weighted IR images were preprocessed to include only voxels with intensity values above 50 and lowpass-filtered to reduce noise by a 3x3 voxel mask. To get the intensity difference image, the after heating images (Step 3) were subtracted from the reference images (Step 1).

2.3.2 Verification of T 1-intensity method using cylindrical phantoms

To verify that small temperature changes could be detected using this relative T1-intensity method, two cylindrical approximately 900-gram agar phantoms were constructed in plastic containers (Ø 10 cm). First cylindrical phantom was heated slowly in a water bath to 31.5°C and the second was kept at room temperature (24.0°C). The containers were then wrapped with 10-mm thick polyethylene cell-foam to restrain the heat exchange with the environment to a minimum.

The heated cylindrical phantom was placed into the scanner so that the cylinder axis was along the bore. Three optic fibres were inserted into the phantom (one in the middle, one to 'right ear' and one to 'nose'). Five axial slices were taken using the IR sequence (parameters as earlier, except: number of slices 5, scanner-reported Estimated SAR 0.8 W/kg, Peak SAR 1.6 W/kg) after which the phantom was allowed to gradually cool towards room temperature. Images were taken at 1°C intervals until the temperature was 27.5°C. The three fibres monitored that the temperature decreased evenly inside the phantom. Finally, the second cylindrical phantom was imaged using the same IR sequence to get a reference at room temperature (cp. Step 1).

The cylindrical phantom images were preprocessed as with the balloon phantom measurements. In addition, voxel averages across each whole volume were calculated.

3. Results

3.1 Evaluation of heating using optic fibre temperature probes

Optic fibres revealed maximally 0.60°C increase at electrode site EOG during a 30-minute GRE-EPI scan (Figure 2). The subsequent SPGR scan increased the temperature by additional 0.14°C, and, despite increased heat exchange with the environment, the high-SAR IR scan by further 0.38°C.

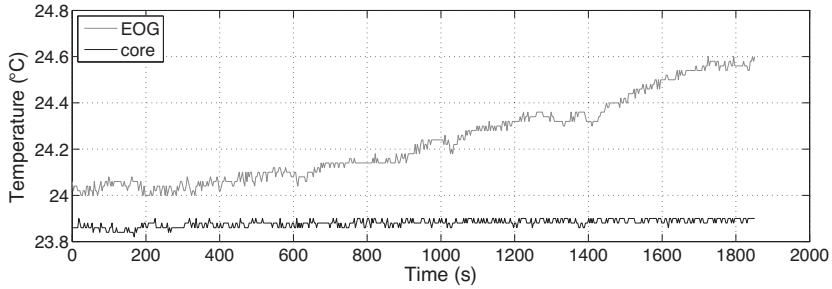

Figure 2 Temperature inside the balloon phantom and at electrode site EOG during 30-minute GRE-EPI measured with optic fibres. Room temperature (24.0^{o}C).

3.2 Evaluation of heating using relative T1-intensity method

Temperature increased only in the proximity of the balloon phantom surface, and no hot spots could be detected (see Figure 3). The dashed line represents the average scalp-to-cortex distance of 13.8 mm (Krakow et al., 2000) from the surface of the phantom. The scale shown does not represent temperature but the difference in signal intensity before (Step 1) and after heating (Step 3)(See Table 1).

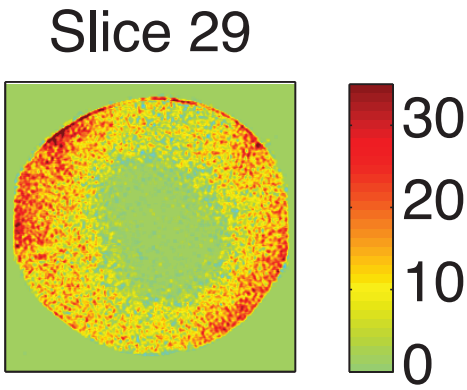

Figure 3 Subtraction MR image of balloon phantom: signal intensity difference before and after FLAIR. Red denotes temperature increase. Colour intensity scale is arbitrary. Dashed line represents average scalp-to-cortex distance from surface.

The intensity difference measured from the cylindrical phantoms increased consistently with temperature (Figure 4).

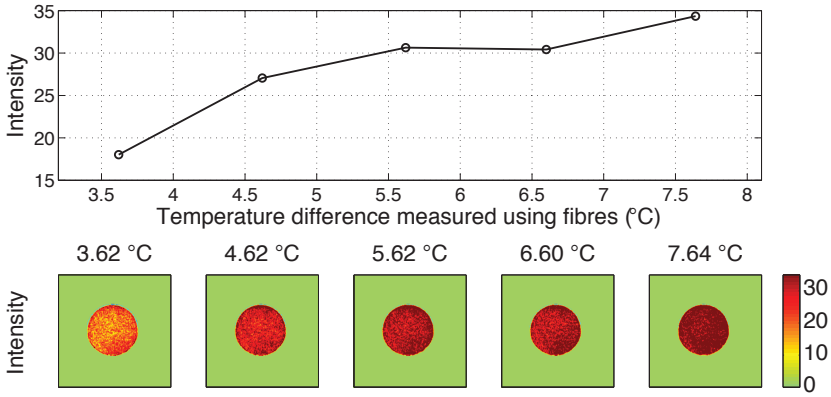

Figure 4 Verification of relative T1-intensity method using cylindrical phantoms (Ø 10 cm). Subtraction MR images vs. temperature difference measured with optic fibres. Above: averaged intensity change over a volume, below: subtraction MR image of slice number 2. Reference at room temperature (24.00C). Colour intensity scale is arbitrary but equivalent with the scale in Figure 3.

4. Discussion

RF induced heating of implants or EEG electrodes can cause serious injury. Although many EEG manufacturers proclaim their products as MR compatible, it is important to always test the whole EEG system within the local MRI scanner since there can be significant differences between the EEG electrode configurations and the scanner RF energy transmission patterns. Our simple safety evaluation procedure complements the previously used local optic fibre temperature measurements with relative temperature maps within a phantom.

The temperature maps were calculated from the relative intensity changes of T1-weighted MR images. There are two main problems with this approach. First, this method can only monitor temperature changes that occur over a time period of minutes. The optic fibres provide better time resolution but only local temperature readings. In addition, the cooling effect of blood flow is not accounted for in phantom experiments.

Second, absolute temperature maps cannot be obtained since the scanner instabilities related to B0 drift, gradient drift, and RF stability can affect the overall image intensity. Our verification experiments with the cylindrical phantoms did show consistent increases in signal intensity difference with temperature, although the relationship was not strictly linear. The cylindrical phantoms were also smaller than the balloon phantom and thus we dare not use the verification measurements as reference temperature scale with the balloon phantom. Nevertheless, any local intensity changes obtained using this relative T1-intensity method should reveal hot spots.

If hot spots were detected, their nature should be evaluated more closely, for example by repeating the T1-weighted imaging sequence several times, or preferably by employing T1 dependent MR thermometry methods such as those described in (Gowland and Stevenson, 2003). The usage of other MR thermometry methods might be limited in the case of implants or electrodes due to susceptibility artefacts in MR images.

The agar-saline gel only approximates the heterogeneous tissues of the human head. The dielectric properties of our gel are quite close to those of blood (ε_{blood}=73, σ_{blood}=1.25 S/m at 128 MHz (Federal Communications

Commission, 2008)). The balloon phantom also experienced some gradual flattening and liquefaction due to gravity and balloon pressure. This could affect the temperature map readings near the surface but unlikely within the phantom.

The SAR monitor of the scanner should not be used as such when determining safe imaging sequences, because local inhomogeneities of the magnetic field caused by the EEG system are not accounted for in SAR limits mentioned in (ICNIRP, 2004). There can also be significant differences between the reported SAR values of different MR systems and resulting temperature increases near implants (Baker et al., 2004). Nonetheless the SAR monitor can be used as a tool for guidelines in a local MRI facility.

After the described safety evaluation procedure, the safety board of our 3-T MRI scanner facility approved the use of three relatively low-SAR sequences: localizer, SPGR and GRE-EPI, each with a precautionary Peak SAR limitation of 1 W/kg with maximum scanning durations of 2, 30 and 15 minutes, respectively. In addition, to ensure subject safety, the users are required to follow a strict safety protocol.

Acknowledgements

We thank Tim Toivo and Tommi Toivonen at Finnish Radiation and Nuclear Safety Authority STUK; Leonardo Angelone at Athinoula A. Martinos Center for Biomedical Imaging, MA, USA; Marita Kattelus, Antti Tarkiainen, and Riitta Hari at AMI Centre, Aalto University, Finland; Iiro Jääskeläinen and Laura Kauhanen at Department of Biomedical Engineering and Computational Science, Aalto University, Finland, for the practical measurements and precious advice.

The study was funded by the Academy of Finland, Centers of Excellence Programme 2006–2011. I.A.n.T. was supported by the Graduate School of Electrical and Communications Engineering, TKK, Finland.

References

Angelone LM, Potthast A, Segonne F, Iwaki S, Belliveau J, Bonmassar G. Metallic electrodes and leads in simultaneous EEG-MRI: Specific absorption rate (SAR) simulation studies. Bioelectromagnetics 2004;25:285–295.

Angelone LM, Vasios CE, Wiggins G, Purdon PL, Bonmassar G. On the effect of resistive EEG electrodes and leads during 7 T MRI: simulation and temperature measurement studies. Magn Reson Imaging 2006;24:801–812.

Baker KB, Tkach JA, Nyenhuis JA, Phillips M, Shellock FG, Gonzalez-Martinez J, Rezai AR. Evaluation of specific absorption rate as a dosimeter of MRI-related implant heating. J Magn Reson Imaging 2004;20:315–320.

Bloembergen N, Purcell E, Pound RV. Relaxation effects in nuclear magnetic resonance absorption. Phys Rev 1948;73:679–712.

Carmichael DW, Thornton JS, Rodionov R, Thornton R, Ordidge ARJ, Allen PJ, Lemieux L. Feasibility of simultaneous intracranial EEG-fMRI in humans: A safety study. Neuroimage 2010;49:379-390.

de Senneville BD, Quesson B, Moonen C. Magnetic resonance temperature imaging. Int J Hyperthermia 2005;21:515–531.

Dempsey MF, Condon B. Thermal injuries associated with MRI. Clin Radiol 2001;56:457–465.

Ehses P, Fidler F, Nordbeck P, Pracht ED, Warmuth M, Jakob PM, Bauer WR. MRI thermometry: Fast mapping of RF-induced heating along conductive wires. Magn Reson Med 2008;60:457-61.

Federal Communications Commission, URL: http://www.fcc.gov/fcc-bin/dielec.sh (18 June, 2008).

Gowland PA, Stevenson VL. T_1: the longitudinal relaxation time. In: Tofts P, editor. Quantitative MRI of the Brain: Measuring Changes Caused by Disease, chapter 5. John Wiley & Sons Ltd., 2003;111–142.

ICNIRP. International Commission on Non-Ionizing Radiation Protection (ICNIRP). Guidelines for limiting exposure to time-varying electric,

magnetic, and electromagnetic fields (up to 300 GHz). Health Phys 1998;74:494–522.

ICNIRP. International Commission on Non-Ionizing Radiation Protection (ICNIRP). Medical magnetic resonance (MR) procedures: Protection of patients. Health Physics 2004;87:197–216.

Krakow K, Allen PJ, Symms MR, Lemieux L, Josephs O, Fish DR. EEG recording during fMRI experiments: Image quality. Hum Brain Mapp, 2000;10:10-15.

Lazeyras F, Zimine I, Blanke O, Perrig SH, Seeck M. Functional MRI with simultaneous EEG recording: Feasibility and application to motor and visual activation. J Magn Reson Imaging 2001;13:943–948.

Lemieux L, Allen PJ, Franconi F, Symms MR, Fish DR. Recording of EEG during fMRI experiments: Patient safety. Magn Reson Med 1997;38:943–952.

Meriläinen V. Magnetic resonance imaging with simultaneous electroencephalography recording: safety issues. Master's thesis, Helsinki University of Technology TKK, Finland, 2002.

Mirsattari SM, Lee DH, Jones D, Bihari F, Ives JR. MRI compatible EEG electrode system for routine use in the epilepsy monitoring unit and intensive care unit. Clin Neurophysiol 2004;115:2175–2180.

Mullinger K, Brookes M, Stevenson C, Morgan P, Bowtell R. Exploring the feasibility of simultaneous electroencephalography/functional magnetic resonance imaging at 7 T. Magn Reson Imaging 2008;26:968-77.

Schanne FJ, Chaffin DB. The effects of skin resistance and capacitance coupling on EMG amplitude and power spectra. Electromyography 1970;10:273-286.

Shellock FG. Radiofrequency energy-induced heating during MR procedures: A review. J Magn Reson Imaging 2000;12:30–36.

Shellock FG. Metallic neurosurgical implants: evaluation of magnetic field interactions, heating, and artifacts at 1.5-Tesla. J Magn Reson Imaging 2001;14:295–299.

Shellock FG. Magnetic resonance safety update 2002: implants and devices. J Magn Reson Imaging 2002;16:485–486.

Stevens TK, Ives JR, Klassen LM, Bartha R. MR compatibility of EEG scalp electrodes at 4 Tesla. J Magn Reson Imaging 2007;25:872–877.

Wlodarczyk W, Hentschel M, Wust P, Noeske R, Hosten N, Rinneberg H, Felix R. Comparison of four magnetic resonance methods for mapping small temperature changes. Phys Med Biol 1999;44:607–624.

Aalto-ST 22/2012

ISBN 978-952-60-4959-5 (pdf)
ISSN-L 1799-4896
ISSN 1799-4896
ISSN 1799-490X (pdf)

Aalto University

School of Electrical Engineering & School of Science
www.aalto.fi

BUSINESS +
ECONOMY

ART +
DESIGN +
ARCHITECTURE

SCIENCE +
TECHNOLOGY

CROSSOVER

DOCTORAL
DISSERTATIONS